Design and synthesis of two functional coordination polymers based on 1,1′-bis(3-carboxybenzyl)-4,4′-bipyridinium ligand

Jiali Chen, Yuying Fu, Qiaoyun Liu*, Shoujie Shen, Jinjian Liu*

Key Laboratory of Magnetic Molecules and Magnetic Information Materials of Ministry of Education & School of Chemistry and Materials Science of Shanxi Normal University, Taiyuan 030032, China.

S1. Experimental section

S1.1 Materials and Methods

All chemicals used in the synthesis are purchased from commercial sources and have not been further purified. 1,1′-bis(3-carboxylatobenzyl)-4,4′-bipyridinium)-dichloride ($H_2BcbpyCl_2$) was synthesized according to the literature [1-2]; A Rigaku Ultima IV-185 diffractometer was used to collect X-ray powder diffraction (PXRD) patterns in the 2θ range 5°–50°; A Vario EL III CHNOS elemental analyzer was utilized to perform elemental analysis of C, H and N; A Nicolet 5 DX spectrometer by taking advantage of KBr pellets was made to acquire FT-IR spectra (4000–500 cm^{-1}); A Varian Cary 5000 UV-vis spectrophotometer was used to perform UV-vis diffuse reflectance spectrum at room temperature; A Bruker A 300-10/12 spectrometer was utilized to record electron paramagnetic resonance (EPR) spectrum at room temperature; Photo-luminescence decay lifetimes were measured at room temperature by an Edinburgh Instruments FLS1000 fluorescence spectrometer; A HTG-3 equipment at 30–800 °C was used to perform thermogravimetric (TGA) experiments under N_2 atmosphere at a heating rate of 10 °C·min^{-1} .

S1.2 Synthesis

The mixture of $H_2BcbpyCl_2$ (0.10 g, 0.2 mmol), $Zn(CH_3COO)_2·2H_2O$ (0.044 g, 0.2 mmol) and *m*-H_2BDC (0.033 g, 0.2 mmol) for **1** / H_4BTEC (0.050 mg, 0.2 mmol) for **2** was dissolved in a mixture of ethanol (4 mL), deionized water (2 mL) and *N*, *N*-dimethylformamide (4 mL). Subsequently, the resulting mixture was transferred to the 25 mL teflon reactor and heated at 90 ℃ for 60 h under sealed conditions. Turn off the oven and allow the mixture in the reactor to slowly cool to room temperature, then transfer to a beaker and filter to obtain yellow crystals for **1** and light blue crystals for **2**. Yield for **1**: 33 %, based on $H_2BcbpyCl_2$. Elemental analysis (%): Anal. Calcd. for $C_{21}H_{14}ZnNO_6$: C, 57.09; H, 3.19; N, 3.17 %. Found: C, 57.05; H, 3.16; N, 3.12 %. IR (KBr, cm^{-1}): 3754, 3374, 2021, 1900, 1614, 1467, 1382, 1230, 1172, 1016, 890, 788, 725, 564 (Fig. S1b). Yield for **2**: 40 % (based on $H_2BcbpyCl_2$). Elemental analysis (%): Anal. Calcd. for $C_{18}H_{13}ZnNO_7$: C, 51.38; H, 3.11; N, 3.33 %. Found: C, 51.22; H, 3.08; N, 3.31 %. IR (KBr, cm^{-1}): 3740, 3378, 3133, 2021, 1909, 1618, 1461, 1372, 1233, 1175, 1018,

891, 784, 569 (Fig. S1c).

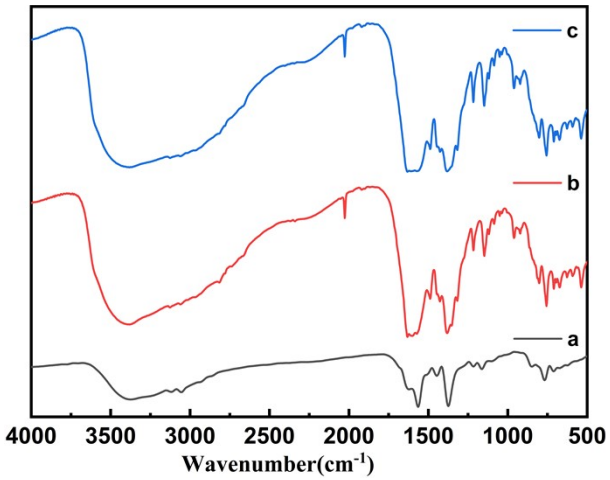

Fig. S1. FT-IR spectra of $H_2BcbpyCl_2$ (a), **1** (b) and **2** (c)

Thermogravimetric analysis (TGA) measurement of **1** and **2** was performed to investigate the thermal stability (Fig. S2). The thermal decomposition is mainly divided into the following stages. The weight losses of 10.99 % occurring between 39–232 °C for **1**. The following sharp weight losses of 40.11% in the temperature range of 232–491 °C should attribute to the decomposition of the whole framework. The final stage is the slow weight loss, up to 491 °C, and the final residual products should possibly be metal oxides. For **2**, the first weight losses of 4.68 % occurring between 62–216 °C should correspond to the loss of coordinated water molecules (calcd 4.24 %). The following sharp weight losses of 45.48 % in the temperature range of 216–541 °C is mainly attributed to the decomposition of the whole framework. At last, the final stage is also a slow weight loss, up to 541 °C, and the final residual products are possibly metal oxides.

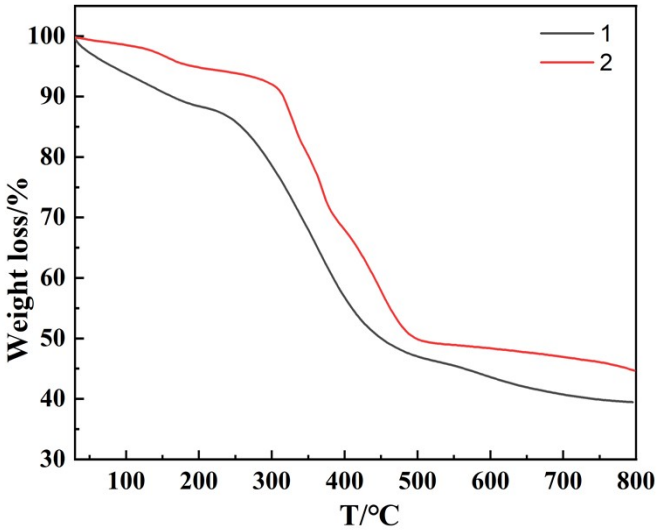

Fig. S2. The TGA test for **1** and **2**

S1.3 X-ray crystallography

According to the analysis, the main peaks of the PXRD spectra of the two newly synthesized

samples were consistent with the simulated data, indicating that solid phase purity is high (Fig. S3). X-ray diffraction data for compounds **1**–**2** was obtained by graphite monochromatic Mo-Kα (λ = 0.71073 Å) on an Oxford Gemini diffractometer at 293 K. The SCALE3 ABSPACK scaling algorithm was used for the empirical absorption correction of the spherical harmonics [3]. The Olex2 software was used to solve and refine the structure on F^2 by direct method and full matrix least squares calculations [4]. All non-hydrogen atoms were anisotropically refined. Table 1 lists the crystallographic data for **1**–**2**, which gives a clear indication of the selected bond lengths and bonds angles.

S1.4 **Kinetic rate calculations**

The kinetic rate constants were calculated according to the determination provided in the literature [5]. The obtained data were processed according to the following formula:

$$ln\frac{I_\infty - I_0}{I_\infty - I_t} = \boldsymbol{kt}$$

where k is the first-order rate constant, and I_0, I_t, and I_∞ refer to the observed emission intensity at 468 nm data at the beginning, versus time and at the end of the reaction, respectively.

S1.5 **Tauc equation**

The Band gaps were calculated from UV-Vis spectra according to the determination provided in the literature [6]. The obtained data were processed according to the following equations:

$$(\alpha h\gamma)^{1/m} = \mathbf{B}(h\gamma - \mathbf{E_g})$$

Direct band gap : m = 1/2; Indirect band gap : m = 2.

where α is the absorption coefficient, **B** is the constant, $h\gamma$ is the photon energy, (γ is the incident photon frequency, h= 4.1356676969 × 10^{-15} eV·s, $\mathbf{E_g}$ represents the semiconductor band gap width (band gap).

References

[1] J. J. Liu, Y. W. Lu, W. B. Lu, *Dyes Pigments,* 2020; **182**, 108631.

[2] S. M. Chen, Y. Ju, H. Zhang, Y. B. Zou, S. Lin, Y. B. Li, S. Q. Wang, E. Ma, W. H. Deng, S. C. Xiang, B. L. Chen and Z. J. Zhang, *Angew.* 2023, **62**, e202308418.

[3] G. Sheldrick, A short history of SHELX, *Acta Cryst. Sect. A.* 2008; **64**, 112-122.

[4] O.V. Dolomanov, L.J. Bourhis, R.J. Gildea, J.A. Howard, H. Puschmann, *J. Appl. Crystallogr.* 2009; **42**, 339 - 341.

[5] Z. Y. Li, J. Z. Guo, F. H. Xiang, Q. J. Lin, Y. X. Ye, J. D. Zhang, S. M. Chen, Z. J. Zhang, S. C. Xiang, *CrystEngComm,* 2018; **20**, 7567-7573.

[6] S. L. Li, Y. Shen,W. Yang, Y. J. Wang, Z. K. Qi, J. Zhang,and Xian-Ming Zhang, *Chin. J. Chem.* 2022; **40**, 351-356.

Table S1. Selected bond lengths (Å) and bond angles (°) for **1**–**2**

Compound **1**			
Zn(1)–O(5)	1.989(2)	Zn(1)–O(6)	1.961(3)
Zn(1)–O(3)	1.950(3)	Zn(1)–O(1)	2.116(3)
Zn(1)–O(2)	2.238(3)		
O(5)–Zn(1) –O(1)	143.92(12)	O(5)–Zn(1) –O(2)	86.47(12)
O(6)–Zn(1) –O(5)	100.11(11)	O(6)–Zn(1) –O(1)	100.60(12)
O(6)–Zn(1) –O(2)	135.09(14)	O(3)–Zn(1) –O(5)	95.57(11)
O(3)–Zn(1) –O(6)	110.34(12)	O(3)–Zn(1) –O(1)	104.41(13)
O(3)–Zn(1) –O(2)	113.15(14)	O(1)–Zn(1) –O(2)	58.18(11)
Compound **2**			
Zn(1)–O(3)	2.048(2)	Zn(1)–O(6^1)	1.994(4)
Zn(1)–O(2)	1.972(3)	Zn(1)–O(4)	1.953(3)
Zn(1)–O(7^1)	2.029(8)		
O(6^1)–Zn(1) –O(3)	84.80(12)	O(6^1)–Zn(1) –O(7^1)	48.2(2)
O(2)–Zn(1) –O(3)	104.77(10)	O(2)–Zn(1) –O(6^1)	130.08(15)
O(2)–Zn(1) –O(7^1)	91.18(19)	O(7^1)–Zn(1) –O(3)	125.2(3)
O(4)–Zn(1) –O(3)	104.81(17)	O(4)–Zn(1) –O(6^1)	128.18(19)
O(4)–Zn(1) –O(2)	97.15(16)	O(4)–Zn(1) –O(7^1)	125.0(3)

Table S2. The hydrogen bond lengths (Å) in **1**–**2**

Compound **1**			
C(9)–H···O(1)	2.562	C(12)–H···O(2)	2.527
C(22)–H···O(3)	2.465	C(17)–H···O(4)	2.537
C(22)–H···O(5)	2.450	C(3)–H···O(5)	3.384
C(2)–H···O(6)	2.890	C(6)–H···O(6)	3.545
C(19)–H···O(6)	2.484		
Compound **2**			
C(3)–H···O(1)	2.605	C(3)–H···O(6)	2.367
C(4)–H···O(2)	2.677	C(8)–H···O(6)	2.954
C(9)–H···O(3)	3.533	C(9)–H···O(5)	2.795
C(9)–H···O(6)	2.565	C(18)–H···O(6)	2.932
C(18)–H···O(20)	3.329	O(3)–H···O(1)	2.892

O(3)–H···O(4)	3.289	O(3)–H···O(6)	2.781
O(3)–H···O(20)	3.502		

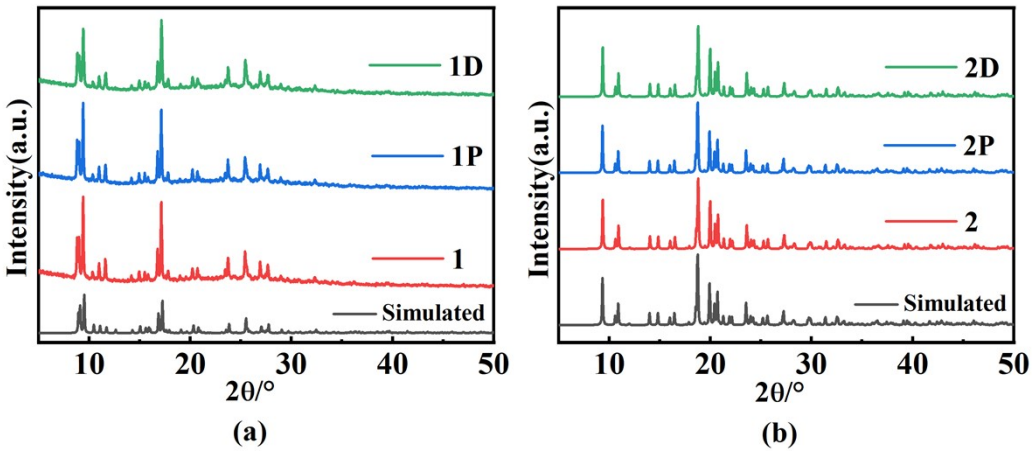

Fig. S3. The PXRD spectra before and after irradiation for **1** (a) and **2** (b)

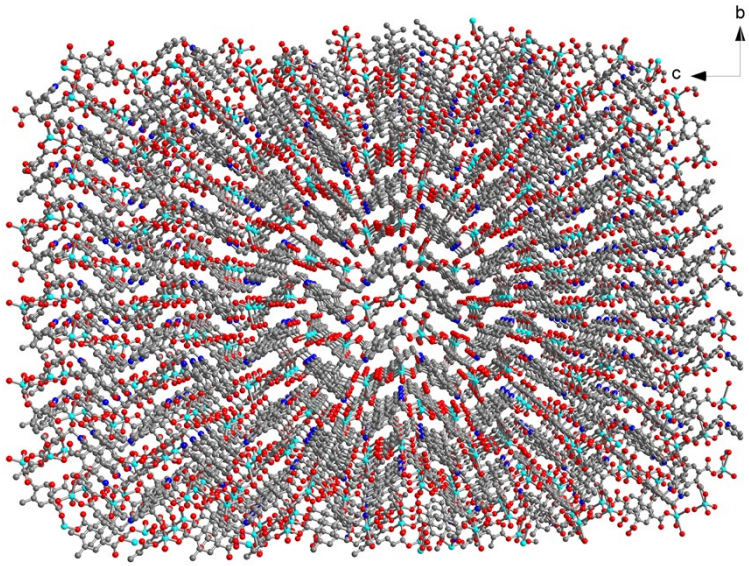

Fig. S4. 3D framework diagram of **2**

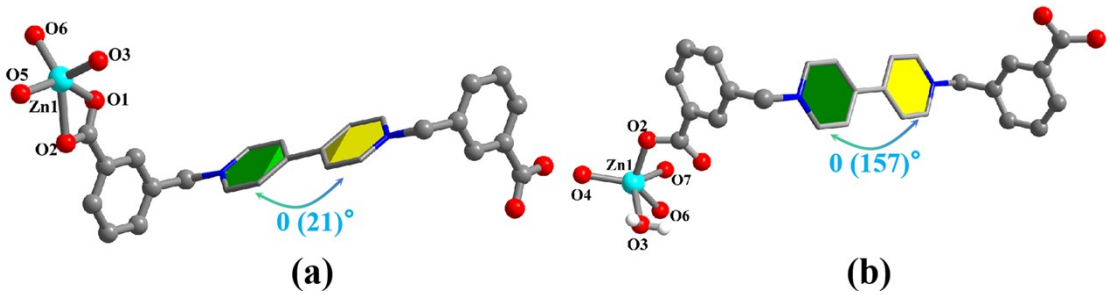

Fig. S5. Dihedral angles between two adjacent pyridyl planes in **1** (a) and **2** (b)

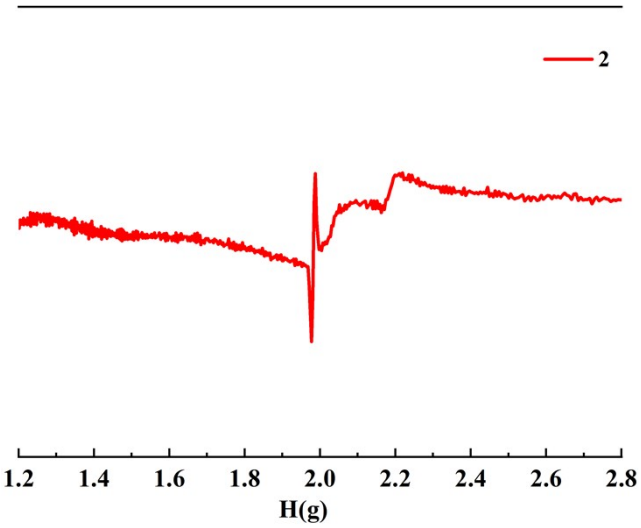

Fig. S6. The EPR spectra before UV irradiation for **2**

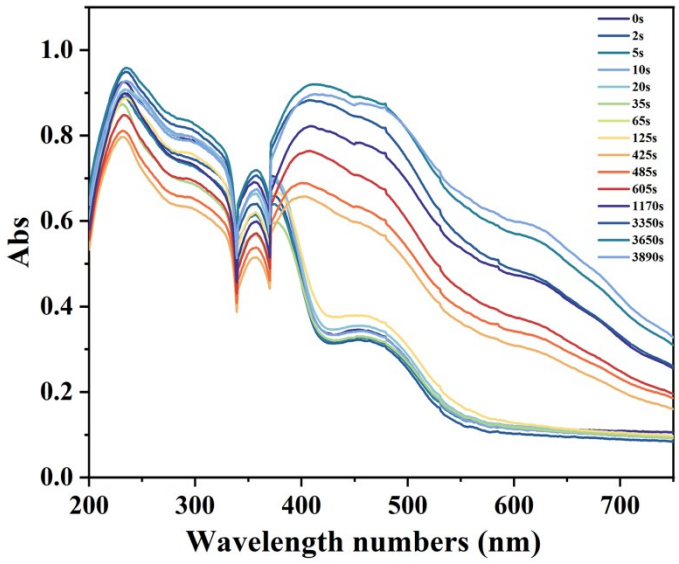

Fig. S7. UV–vis spectra before and after UV-light irradiation for $H_2BcbpyCl_2$

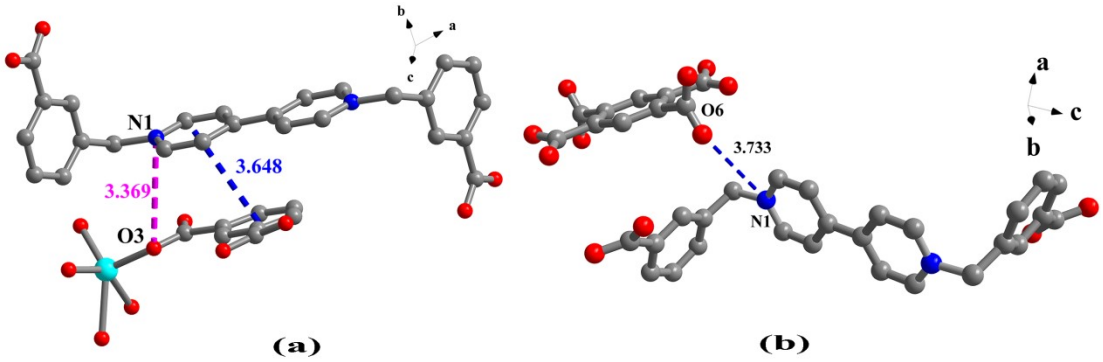

Fig. S8. The electron transfer distance and π···π distance for **1** (a); The electron transfer distance for **2** (b)

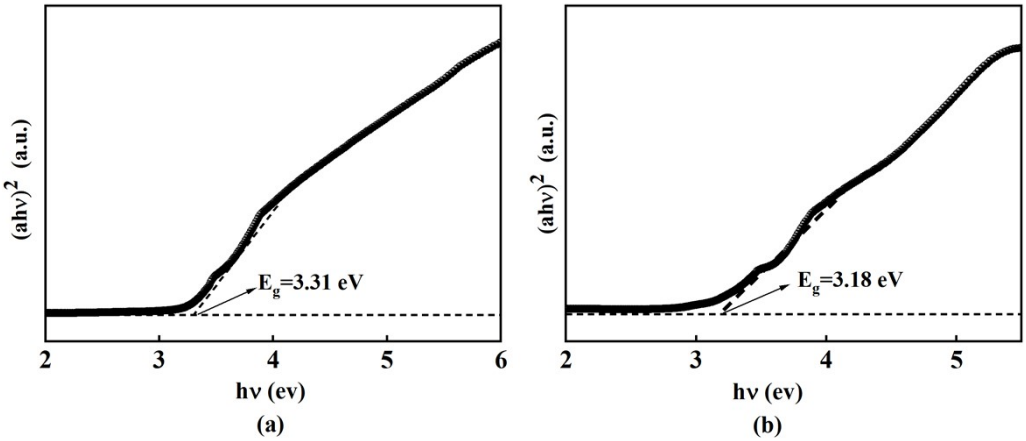

Fig. S9. UV–vis spectra band gap for **1** (a) and **2** (b)